Title

The role of Müller cells in tractional macular disorders: an optical coherence tomography study and physical model of mechanical force transmission

Journal

British Journal of Ophthalmology, 104(4)

ISSN

0007-1161

Authors

Govetto, Andrea
Hubschman, Jean-Pierre
Sarraf, David
et al.

Publication Date

2020-04-01

DOI

10.1136/bjophthalmol-2019-314245

Peer reviewed

Abstract

Purpose: To explore the role of foveal and parafoveal Müller cells in the morphology and pathophysiology of tractional macular disorders with a mathematical model of mechanical force transmission.

Design: Retrospective, consecutive, observational case series.

Methods: Spectral-domain optical coherence tomography (SD-OCT) images of tractional lamellar macular holes and myopic foveoschisis patients were reviewed and analyzed. The structure of foveal and parafoveal Müller cells was analyzed with a simplified mathematical model of force transmission. Parafoveal *z-shaped* Müller cells were modelled as a structure composed of three rigid rods, named R1, R2 and R3. The angle formed between the rods was referred to as θ. R1, R2 and R3 lengths as well as the variation of the angle θ were measured and correlated with best corrected visual acuity (BCVA).

Results: In tractional lamellar macular holes, there was a significant reduction of the angle θ toward the foveal center (p<0.001). By contrast, there were no significant differences in θ in myopic foveoschisis (p=0.570). R2 segments were more vertical in myopic foveoschisis. There was a significant association between lower θ angles at 200µm temporal and nasal to the fovea and lower BCVA (p<0.001 and p=0.005, respectively). The stiffness of parafoveal Müller cells was predicted to be function of the angle θ, and it grew very rapidly as the θ decreased.

Conclusion: Parafoveal Müller cells in the Henle fiber layer may guarantee structural stability of the parafovea by increasing retinal compliance and resistance to mechanical stress. Small values of the angle θ were related to worse BCVA possibly due to damage to Müller cell processes and photoreceptor's axons.

The role of Müller cells in tractional macular disorders: an optical coherence tomography study and physical model of force transmission.

Short title: The role of Müller cells in tractional macular disorders.

Andrea Govetto,[1] Jean Pierre Hubschman,[2] David Sarraf,[3,4] Marta S. Figueroa,[5] Ferdinando Bottoni,[6] Roberto Dell'Omo,[7] Christine A. Curcio,[8] Patrizio Seidenari,[1] Giulia delle Donne,[6] Robert Gunzenhauser,[1] Mariantonia Ferrara,[9] Adrian Au,[3] Gianni Virgili,[10] Antonio Scialdone,[1] Rodolfo Repetto,[11] Mario R. Romano.[9]

1. Oftalmico Hospital, ASST-Fatebenefratelli-Sacco, Milan, Italy.
2. Retina Division, Stein Eye Institute, University of California, Los Angeles, CA, USA.
3. Retinal Disorders and Ophthalmic Genetics Division, Stein Eye Institute, University of California, Los Angeles, CA, USA.
4. Greater Los Angeles VA Healthcare Center, Los Angeles, CA, USA.
5. Ramon y Cajal University Hospital, Alcala' University, Madrid, Spain.
6. Eye Clinic, Department of Clinical Science "Luigi Sacco", Sacco Hospital, University of Milan, Italy.
7. Department of Medicine and Health Sciences, University of Molise, Campobasso, Italy.
8. Department of Ophthalmology and Vision Sciences, University of Alabama, Birmingham, AL, USA.
9. Humanitas University, Eye Unit, Humanitas-Gavazzeni Hospital, Bergamo, Italy.
10. Ophthalmology Department, Careggi University Hospital, University of Florence, Florence, Italy.
11. Department of Civil, Chemical and Environmental Engineering, University of Genoa, Genoa, Italy.

Corresponding Author:

Andrea Govetto

Oftalmico Hospital, ASST-Fbf-Sacco

Via Castelfidardo 15, 20121, Milan, Italy

Telephone: +390263632232, Fax: +390263632670

Email: a.govetto@gmail.com

Introduction:

Despite extensive histologic study and research, the precise anatomical and microstructural glial composition of the human fovea has been a matter of conjecture over the last decades. This debate has focused on the presence or absence of Müller Cells in the central fovea.

More than a century ago, Rochon-Duvigneaud described a small circular island, less than 100µm in diameter in the central fovea of humans and primates, that is exclusively comprised of approximately 2000 of the thinnest cone photoreceptors.[1,2] This so-called "central foveal bouquet" was originally described without mention of any glial component. However, in 1969, based on the results of an electron microscopic study in a human autopsy eye, Yamada proposed the presence of a specific subtype of Müller cells in the very central fovea providing structural support to the foveal cones.[2] Yamada's hypothesis was later interpreted by Gass as a central "plug" of specialized Müller cells in the shape of an inverted cone. Gass referred to this structure as the "Müller cell cone".[3]

The existence of a central distinctive population of Müller cells was later supported by a histopathology study by Syrbe et al.[4] Some authors suggested that central foveal Müller cells efficiently transmit mechanical forces to the central cones, resulting in outer retinal abnormalities and macular holes.[5]

Müller Cells in the parafoveal region, unlike the central inverted plug, display a remarkable "*z-shaped*" anatomical configuration, which has long being known since Ramon y Cajal.[6] The horizontal part of the z-shaped Müller cells contributes to the Henle's fiber layer (HFL) comprised of bundles of cone and rod photoreceptor axons terminating in the pedicles and spherules, respectively, that form synapses in the retinal outer plexiform layer (OPL). This characteristic histological configuration is the result of foveal pit development during which photoreceptor inner segments migrate inward and ganglion cells migrate outward.[7]

The Henle fiber layer is often considered a structural weak point of the retina as it is the preferred location of intraretinal "splitting" typically seen in tractional disorders such as tractional lamellar macular hole and myopic traction maculopathy.[8,9] In these clinical entities, inner and outer retina are connected by characteristic intraretinal "bridges" of tissue, which may correspond to stretched Müller cells processes together with photoreceptor's axons.[8-11]

Despite the seminal role of foveal and parafoveal Müller cells in tractional macular disorders, their mechanical behavior under stress has not yet been exhaustively elucidated. Further, the clinical course of schitic conditions cannot be clearly explained by current pathophysiological knowledge.

In this study, we incorporate novel clinical observations with optical coherence tomography supported by a mathematical model to explore the role of foveal and parafoveal Müller cells in the morphology and pathophysiology of specific tractional macular disorders. We propose that the distinctive "*z-shaped*" configuration of parafoveal Müller cells may increase retinal compliance to mechanical stress, protecting parafoveal photoreceptors from tractional forces.

Methods:

Study Design:

This was a retrospective, observational and multicenter study designed according to the tenets of the Declaration of Helsinki. The study protocol was separately approved by the institutional review boards of each of the participating centers: the Fatebenefratelli-Oftamico Hospital (Milan, Italy), the Luigi Sacco University Hospital (Milan, Italy), the Humanitas-Gavezzeni University Hospital (Bergamo, Italy), the Ramon y Cajal University Hospital (Madrid, Spain) the University of Molise (Campobasso, Italy) and the Stein Eye Institute, University of California Los Angeles (Los Angeles, USA).

Electronic and paper records of all patients diagnosed with tractional lamellar macular hole and myopic foveoschisis evaluated at the participating centers between January 1, 2010 and October 1, 2018 were reviewed and analyzed. In all participating European centers cases were identified using administrative lists and institutional patient databases, while at the Stein Eye institute cases were identified using imaging databases or by a medical billing record search, using the International Statistical Classification of Diseases and Related Health Problems, Ninth Revision (ICD-9) diagnosis code 362.56 for macular pucker and 360.21 for progressive (high) myopia.

Inclusion criteria included the presence of tractional lamellar macular hole or myopic foveoschisis, diagnosed according to previously published criteria, in patients with a minimum follow up of six months.[4]

Exclusion criteria are listed in Table 1.

Hypothesis: a simplified model of foveal and parafoveal z-shaped Müller cells:

For the purpose of this study, parafoveal z-shaped Müller cells were modelled as the structure illustrated in Figure 1. The cell consisted of three rigid rods, connected through two flexible or rotating hinges. The three rods were labelled as R1, R2 and R3, and their lengths L_1, L_2 and L_3.

In this depiction, R1 corresponded to the vertical part of the Müller cell comprised between the OPL and the internal limiting membrane (INL); R2 corresponded to the horizontal part of the Müller cell located within the Henle fiber layer; R3 corresponded to the vertical part of the Müller cell located between the outer nuclear layer (ONL) and the external limiting membrane (ELM). Of note, in Newtonian physics the term “vertical” refers to the direction of the force of gravity, which is not the case of the presented model. However, in this study the terms “vertical” and “horizontal” were used for the sake of simplicity; “vertical” referred to a direction orthogonal to the retinal pigment epithelium (RPE), whether “horizontal” referred to a direction parallel to the RPE, as seen with spectral-domain optical coherence tomography (SD-OCT).

The angle formed between the rods was referred to as θ and its amplitude varied between 0° and 90° depending on the hinge rotation (Figure 1 left, middle-left, middle-right). In the “relaxed” configuration, R2 was horizontal, with the angle θ equal

to 90° (Figure 1, left) while in a completely "stretched" configuration, R2 was vertical and aligned with R1 and R3, with $\theta = 0°$ (Figure 1, middle-right)

The model was based on the following assumptions: the bottom end of rod R3 is fixed and both R1 and R3 maintain vertical orientations.

By contrast to the parafoveal area, foveal Müller cells were depicted as a single rigid rod (R) with a length L and without any connecting hinge. The mechanical behavior of foveal Müller cells was considered equivalent to that of a fully stretched parafoveal z-shaped Müller cells (i.e. $\theta = 0°$, Figure 1, right).

Clinical assessment and spectral-domain optical coherence tomography analysis:

At presentation and at the end of the follow-up, all patients underwent a complete ophthalmologic assessment, which included slit-lamp biomicroscopy and dilated fundus examination. Snellen best corrected visual acuity (BCVA) was obtained and converted into the logarithm of the minimum angle of resolution (logMAR) for statistical analysis.

The Heidelberg Spectralis SD-OCT device (Heidelberg Engineering, Heidelberg, Germany) with active eye-tracking technology was employed to image all included eyes. All SD-OCT scans were analyzed with the Heidelberg Eye Explorer (version 1.8.6.0) using the HRA/Spectralis Viewing Module (version 5.8.3.0).

All SD-OCT images were acquired using a single high-definition horizontal B-scan at 30 degrees and were qualitatively and quantitatively evaluated by experienced retinal specialists.

In all cases of the SD OCT analysis, quantitative measurements were made as illustrated in Figure 2. The schitic "bridges" of tissue were assumed to be comprised by the Henle fiber layer (including the z-shaped Müller Cells)[9] and corresponded to the R2 segment of the modeled parafoveal z-shaped Müller cell previously described. The R1 segment corresponded to a vertical line traced from the ILM to the beginning of the R2 segment under the OPL. The R3 segment corresponded to a vertical line traced from the end of the R2 segment below the Henle fiber layer to the ELM.

The R segment length L, corresponding to foveal Müller cells, was measured if a vertical "bridge" of tissue was encountered within 50µm nasal or temporal to the fovea.

In all cases R, R1, R2 and R3 lengths L, L_1, L_2 and L_3 were measured using the "caliper" function of the Heidelberg proprietary software.

In the parafovea, such measurements were repeated at 200µm, 500µm, 1000µm, 1500µm, 2000µm and 3000µm nasal and temporal to the fovea, depending on the horizontal extension of the schisis.

The angle θ was calculated at any measured location using the "angle" tool of Image J version 1.52e open source software. By definition, in R segments θ was considered equal to 0°.

Quantitative analysis of SD-OCT scans included the evaluation of the outer retinal bands including the ellipsoid zone band and the ELM (preserved or disrupted) and grading of tractional outer retinal abnormalities was performed according to prior

published system and included the cotton ball sign, foveolar detachment and acquired vitelliform lesion.[5] The band's integrity was assessed by categorical descriptors (i.e. Yes/No).

All quantitative measurements and qualitative analysis were repeated both at presentation and at the end of the follow-up period.

Statistical analysis:

Descriptive statistics were calculated for all variables of interest. Mean and standard deviation values were calculated for continuous variables, while frequency and percentage were calculated for categorical variables. Paired *t*-test were used to compare the angle θ at different macular locations. Spearman correlation coefficient was used to investigate the association between variables. Linear mixed models were used to explore the change of the angle θ during follow-up. Stata 15.1 software (StataCorp, College Station, TX) was used for all statistical analyses.

Results

In total 96 eyes from 93 patients, of which 74 were females and 22 were males, met the inclusion criteria and were enrolled and analyzed in the study. Mean age of the study population was 70 ± 11 years (range 35-89), while mean follow up was 24.1 ± 24.5 months (range 3-106).

Tractional lamellar macular holes were diagnosed in 85 out of 96 eyes (88.5%), while the remaining 11 eyes (11.5%) were diagnosed with myopic foveoschisis.

At presentation, mean visual acuity was 0.25 ± 0.28 logMAR (20/35 Snellen Equivalent), ranging between 0 and 1.5 logMAR (20/20 and 20/600 Snellen Equivalent). BCVA was significantly higher in eyes with tractional lamellar macular holes (0.21 ± 0.24 LogMAR, 20/32 Snellen Equivalent) versus those with myopic foveoschisis (0.60 ± 0.38 logMAR, 20/80 Snellen Equivalent), p=0.001.

Baseline SD-OCT qualitative analysis and associations with BCVA:

At presentation, tractional abnormalities of the central foveal bouquet were identified in 4 out of 11 eyes (36.4%) with myopic schisis, in which a foveolar detachment was diagnosed in all cases. These outer retinal abnormalities were encountered in only 3 of 85 eyes with tractional lamellar macular hole (3.5%) and the difference between the two subgroups was statistically significant (p<0.001).

Similarly, EZ and ELM disruption in the central fovea was more frequent in the myopic foveoschisis group, present in 5 out of 11 eyes (45.5%). Only 1 out of 85 eyes with tractional lamellar macular hole (1.2%) displayed this abnormality and the subgroup comparison was again statistically significant (p<0.001).

None of the eyes diagnosed with tractional lamellar macular hole displayed EZ and ELM disruption in the parafoveal area at any measured location. By contrast, parafoveal outer retinal disruption was significantly higher in myopic foveoschisis at any measured location (p<0.001).

The presence of a vertical segment R (defined as angle $\theta = 0°$ as shown in Figure 1, middle, right) in the central fovea was noted in the majority of eyes with myopic foveoschisis (8 out of 11, 73%). By contrast, the segment R was present in only 29 out of 85 tractional lamellar macular holes (34.1%), and this difference was statistically significant (p=0.013).

Qualitative SD-OCT analysis is summarized in Table 2.

Baseline SD-OCT quantitative analysis and association with BCVA:

In tractional lamellar macular holes, there was a significant reduction in θ amplitude toward the foveal center (p<0.001). By contrast, there were no significant differences in the angle θ in myopic foveoschisis, at any measured location (p=0.57). In other words, in tractional lamellar holes the amplitude of θ increased farther from the foveal center and decreased closer to the foveal center, while in myopic foveoschisis this angle amplitude was similar at any measured location.

Globally, θ was lower (less steep) at any measured location in myopic foveoschisis when compared to tractional lamellar macular holes. Consequently, R2 segments were more vertical in myopic foveoschisis.

In the study population, there was a significant association between lower θ angles at 200 µm temporal and nasal to the fovea and lower BCVA (p<0.001 and p=0.005, respectively).

The central R segment was significantly longer in myopic foveoschisis (p<0.001). Similarly, R2 segment was significantly longer in myopic foveoschisis if compared to tractional lamellar macular hole, at any measured location (p=0.015). Contrastingly, R1 and R3 lengths were not significantly different between the two subgroups (p>0.1), at any measured location. Peak L_2 was 471µm in myopic foveoschisis and 300µm in tractional lamellar macular hole, both measured at 500µm from the foveal center.

Baseline quantitative analysis is summarized in table 3 and 4.

Longitudinal functional and anatomical analysis:

At the end of the mean follow-up of 24.1 ± 24.5 months, there were no significant differences in BCVA in the study population, if compared to baseline (p=0.900).

Similarly, there were no significant differences in R, R1, R2 and R3 lengths at the end of the follow-up period at any measured location (p>0.05).

The angle θ remained roughly stable over the follow-up period. Linear mixed models did not find any significant trend in the angle θ longitudinal change.

A simplified mathematical model of Müller cell's stiffness:

It is assumed that the hinges have an elastic modulus equal to γ, so that if an infinitesimal moment dM is applied to the hinge it produces a variation $d\theta$ of the angle θ formed by the two rods, linked to dM by the following expression:

$$dM = \gamma d\theta. \quad (1)$$

The stiffness of the structure in the z direction was calculated as a function of the angle θ and the length of the rod R2, L_2. The cell was modeled as an equivalent elastic spring, so that if an infinitesimal force dF is applied the top of the rod R1 the length of the structure varies by a quantity dl according to the following spring law:

$$K(\theta, L_2)dl = dF, \quad (2)$$

where the stiffness K depends on the angle θ and on the length L_2. Using equation (1) and the notation in Figure 1 we can write:

$$dM = 2\gamma d\theta = -L_2 sin\theta dF, \quad (3)$$

where the factor 2 appears owing to the presence of two springs that we assume to deform equally. From the above expression we obtain:

$$d\theta = \frac{-L_2 sin\theta}{2\gamma} dF. \quad (4)$$

Moreover, $d\theta$ can be linked to dl as:

$$dl = L_2 cos(\theta + d\theta) - L_2 cos(\theta) = -L_2 sin\theta d\theta + O(d\theta^2). \quad (5)$$

Substituting (5) and (4) into (2) we obtain:

$$K = \frac{2\gamma}{L_2^2 sin^2(\theta)}. \quad (6)$$

This shows that the stiffness of the equivalent spring is proportional to the inverse of the square of the length of the rod R2, L_2, and to the inverse of the square of $sin\theta$. The stiffness of the equivalent spring K is plotted in Figure 3, left, normalized with the corresponding value K_{90} for $\theta = 90°$ ($\theta = \pi/2$), as a function of θ. We note that $K/K_{90} = 1/sin^2(\theta)$.

Figure 3, left, shows that cell stiffness grows very rapidly as the angle θ decreases. In particular, K/K_{90} increases to very large values when the angle θ assumes values below approximately 20°. This means that when the cell assumes a stretched configuration, it is much stiffer than when it is highly bent and it is thus likely to transmit much larger tractional forces to the substrate, increasing the risk of detachment.

We also note that, given a certain configuration corresponding to an angle θ, the cell can undergo a maximum extension of $L_2(1 - cos\theta)$ and, therefore, when the cell is already stretched (small values of θ) is has a very small capability of stretching further.

If we assume that the relaxed configuration of the cell corresponds to the angle $\theta = 90°$ ($\theta = \pi/2$) and that the elastic modulus of the hinges is constant (it

does not depend on the angle), the force F corresponding to a certain configuration with angle θ ($\theta < \pi/2$) can be obtained as:

(7)

In Figure 3, right, we plotted the force F (scaled with) as a function of the angle θ. As expected, the behavior is highly nonlinear, owing to the variable stiffness of the cell.

Discussion:

The distinctive anatomical configuration of the fovea and parafovea is the result of the centrifugal displacement of the inner retina and the centripetal displacement of the outer retina and photoreceptors, causing the z-shaped pattern of parafoveal Müller cells.[7-11]

Müller cell processes, together with bundles of unmyelinated cone and rod photoreceptors axons, comprise the Henle fiber layer between the outer nuclear and outer plexiform layers.[10-13] In the parafovea, the Müller cell component of the Henle fiber layer is particularly relevant. In such region, Muller cells may be even equal in number to cones at 1-degree eccentricity.[14,15]

For the purpose of this study, this z-shaped configuration was depicted as a rigid structure formed by three rods (R1, R2 and R3) connected by two rotating hinges. This model parallels the morphology of parafoveal z-shaped Müller cells, as noted in Figure 1.

Importantly, it must be highlighted that, although Müller cells do not represent the exclusive cellular component of the Henle fiber layer, the role of photoreceptors axons was not analyzed in the model. Differently from Müller cells, photoreceptor axons end abruptly in the OPL, where they synapse with bipolar cells.[10] Therefore, their role in the structural stability of the retina was considered to be marginal.

Previous works have investigated the physical properties of retinal Müller cells by exploring their empirical contractility in-vitro.[16-21] Nevertheless, the approach of the present study was different, as it aimed to predict the mechanical behavior of the cells on the sole basis of their peculiar morphology.

In our study population, comprised of eyes with tractional lamellar macular holes and myopic foveoschisis, Müller cell processes located in the Henle fiber layer displayed a beveled and/or a vertical disposition. This would imply that the cellular component R2, originally horizontal, may rotate until it becomes completely vertical in response to mechanical forces applied over the inner retina (R1). This fact may guarantee high compliance and resistance to mechanical stress.

To quantify how the z-shaped morphology of Müller Cells may absorb and dampen mechanical stresses, we plotted the stiffness of the cell as a function of the angle θ. As illustrated in Figure 3, left, Müller cell stiffness increases rapidly as the angle θ decreases, particularly at values lower than 20°. By contrast, the stiffness significantly decreases as the angle θ approaches 90°. Therefore, in the relaxed configuration (right angles between the three rods) the tension of the cell is minimal,

as well as its capacity to transmit mechanical stress to the photoreceptors. By contrast, in a fully stretched configuration (zero angle between the three rods), the tension is maximal and the cell may transmit significant mechanical stress to the outer retina even as a response to very small displacements of the cell head. That is the case of Müller cells in the central fovea (Müller cell "cone"), which display a vertical orientation, and behave similarly to fully stretched parafoveal Müller cells.

The analysis of angle θ revealed significant differences between eyes with tractional macular holes versus myopic foveoschisis, as depicted in Figure 4. In the former, the angle θ progressively decreases toward the foveal center, i.e. it is higher the farther from the fovea (closer to 90°) and smaller closer to the foveal center (closer to 0°). On the other hand, in myopic foveoschisis the angle θ was small (closer to 0°) and with little variation across all the measured locations. This translates into a more vertical orientation of R2 segments in myopic eyes.

Similarly, in tractional lamellar macular hole R2 length L_2 increased progressively toward the center, while in myopic foveoschisis the length L_2 was similar at all measured locations.

These findings suggest that in myopic foveoschisis mechanical forces may be stronger and uniformly distributed over the macular region, while in tractional lamellar macular holes mechanical stresses may be greater over the foveal center. In myopic foveoschisis, the presence of a posterior staphyloma may also contribute to R2 elongation and verticalization.

In previous publications it has been suggested that myopic foveoschisis and tractional lamellar macular holes may be caused by stresses exerted by different vectors i.e. anteroposterior (vertical) forces with myopic foveoschisis and centrifugal (horizontal) forces with tractional lamellar holes.[5,22] However, based on our observations, the vector of the force applied over R1 could not be estimated.

Under the assumption that R1 and R3 maintain a vertical position, the conformation of the system is entirely determined by the value of the angle θ, which defines the orientation of R2. Any R2 orientation can be obtained by applying over R1 either a vertical or horizontal force. Therefore, any R2 conformation and angle θ could derive by infinitely many combinations of vertical and horizontal forces over R1.

In our simplified model, the lengths of R1 and R3 (L_1, L_3) were similar in both tractional lamellar macular holes and myopic foveoschisis, without significant differences among the two subgroups. By contrast, the R2 length i.e. L_2 was significantly longer in myopic foveoschisis, suggesting that there may be greater mechanical stress or tension exerted over R2, the segment of the Müller cell located in the Henle Fiber Layer.

Variations in the angle θ were also functionally relevant, as θ impacted visual acuity. In the study population, smaller θ angles at 200µm nasal and temporal to the central fovea were significantly associated with lower visual acuity. Such an effect was negligible in tractional lamellar macular holes and became significant only when eyes with myopic foveoschisis were included in the analysis.

Although it is unclear how the angle θ may correlate with visual acuity, it can be speculated that highly stretched and stiffer R2 segments may have a greater risk of disrupting the underlying photoreceptors. This is because, as shown by our model,

stiffer cells have very limited capacity of further deforming and stretching and transmit forces very efficiently, which can result in cell break. This fact may be particularly relevant in myopic foveoschisis, characterized by longer more verticalized R2 segments, as in the illustrated case in Figure 5. As Müller cell processes run together with cone and rod axons in the Henle fiber layer, structural damage at this level may compromise the capacity of photoreceptor to synapse in the outer plexiform layer, causing a decrease in visual acuity.

Longitudinal data showed no significant differences in θ and/or in the length of R, R1, R2 and R3 segments, suggesting that such lesions remained morphologically stable over the follow-up period once mechanical equilibrium was reached.

The hypothesis of the "damping" role of the parafoveal Henle fiber layer is supported by previous laboratory studies. It has been shown that glial fibrillary acidic protein (GFAP) may contribute to the biomechanical properties of Müller cells by upregulation of intermediate filaments after mechanical stimulation.[23] As proposed by Bringmann et al., GFAP expression in Müller cells is a very sensitive indicator of stress, and this molecule is constitutively expressed in the OPL and Henle fiber layer.[24] This may signify the presence of ongoing mechanical stress in these layers. Therefore, some authors hypothesized that GFAP distribution may support the assumption that Müller cell processes in the Henle fibers underlie the structural stability of the parafovea.[11]

This study has limitations, including its retrospective design, which may have biased the observations. The orientation of parafoveal Muller cell processes within the Henle fiber layer is slightly oblique as seen with histology, but in our depiction was horizontal for the sake of simplicity. Further, the proposed model may be too simplistic to properly describe mechanical properties on cellular scale. This limitation appears evident if we consider the complexity of the retinal tissue, formed by various interconnected cellular subtypes including the extracellular matrix and blood vessels. Each component may act differently in response to mechanical stress.

In the present study Müller cells were considered as main determinants of force transmission, as they span through almost the whole thickness of the retina. However, throughout their path, Müller cells interact and form connections with other cellular components.[10-13] Therefore, it is assumable that mechanical stress may also be transmitted through the Müller cells to distinct cellular subtypes other than the fotoreceptors. Such complex interactions were not considered in our model.

Strengths of this study include a relatively large study population and a significant follow up analysis of many of the cases. Moreover, the mathematical model proposed helped us understanding the mechanical implications of our clinical findings, based on the SD OCT analysis.

Our analysis did uncover discrepancies in R2 length L_2 between SD-OCT and histological measurements. The Henle fiber's portion of parafoveal Müller cells have been measured by Drasdo et al., who reported a maximum length projected onto the ELM of 536-675µm (nasal to the fovea) and 406-664 µm (temporal to the fovea) in 6 normal maculas of young adults.[25] Previous studies reported shorter maximum lengths in monkey[26] and in non-foveal sections of human eye.[27] In the present work, R2 maximum length was shorter, as it reached a peak of 471µm in myopic

foveoschisis and 300μm in tractional lamellar macular hole. Determining the reasons for these quantitative differences will require further research.

Differently, the qualitative distribution of R2 lengths resembled that seen in histology, as in our measurements L_2 peaked at 500μm to the fovea and then it fell of farther from the foveal center.[25,26]

In the present study, R1, R2 and R3 were modeled as rigid bodies. However, Müller cells in vivo act as elastic solids.[28] Therefore, the intraretinal bridges of tissue seen with SD-OCT may correspond to just a part of the whole R2 segment, as depicted in Figure 6. However, from a geometrical standpoint, our model was consistent with clinical and histology images. This may suggest the existence of cell compartments characterized by a lower bending stiffness, which is where high curvatures are observed (i.e. the elastic hinges). If this is the case, our simple model may reliably reproduce the mechanical behavior of the system.

To conclude, our report explored the possible behavior of foveal and parafoveal Müller cells in response to mechanical forces with the development of a straightforward physical model of force transmission. The stiffness of the Müller cells may dramatically increase at decreasing values of angle θ, which may translate in higher mechanical force transmission to photoreceptors. Such results suggest the key role of Henle fiber layer in maintaining structural stability of the parafovea by increasing retinal compliance and resistance to mechanical stress. Small values of the angle θ were related to worse BCVA possibly due to damage to Müller cell processes and photoreceptor's axons.

Our conclusions are clinically relevant, as they may signify that presynaptic damage to the phoreceptor's axon could potentially contribute to vision loss in schitic disorders. This hypothesis is worth of further investigation to understand how, and to which extent, mechanical stretching of the Henle fiber layer may interrupt or degrade photoreceptor signaling.

Moreover, further larger studies will be necessary to reduce bias. More complex engineering simulations will be key to build accurate mathematical models on the behavior of Müller cells in tractional macular disorders.

ACKNOWLEDGMENTS/DISCLOSURE:

A. Funding/Support: None

B. Financial Disclosures: Andrea Govetto: None; **Jean Pierre Hubschman**: consultant for Alcon (Fort Wort, TX, USA), Allergan (Dublin, Ireland); **David Sarraf**: consultant for Amgen (Thousand Oaks, CA, USA), consultant and speaker for Bayer (Leverkusen, Germany), consultant and researcher for Genentech (San Francisco, CA, USA), researcher for Heidelberg (Heidelberg, Germany), speaker for Novartis (Basel, Switzerland), consultant, researcher and speaker for Optovue (Freemont, CA, USA), researcher for Regeneron (Tarrytown, NY, USA); **Marta S. Figueroa**: consultant for Novartis (Basel, Switzerland), Alcon (Fort Wort, TX, USA), Bayer (Leverkusen, Germany), Allergan (Dublin, Ireland), Hoffman LaRoche (Basel, Switzerland), Zeiss (Oberkochen, Germany); **Ferdinando Bottoni:** consultant for Novartis (Basel, Switzerland), Bayer (Leverkusen, Germany); **Roberto Dell'Omo**: None; **Christine A. Curcio:** Consultant for Genentech (San Francisco, California, USA), Merck (Whitehouse Station, New Jersey, USA) Janssen Cell Therapy (Raritan, New Jersey, USA); research support from Hoffman LaRoche (Basel, Switzerland). **Patrizio Seidenari:** None; **Giulia delle Donne**: None; **Robert Gunzenhauser:** None; **Mariantonia Ferrara**: None; **Adrian Au**: None; **Gianni Virgili**: None; **Antonio Scialdone**: None; **Rodolfo Repetto**: None; **Mario R. Romano:** research grants from Alcon (Fort Wort, TX, USA); DORC (Zuidland, Holland); Baush & Lomb (Rochester, NY, USA); Bayer (Leverkusen, Germany), consultant for Leica (Wetzlar, Germany).

REFERENCES

1. Rochon-Duvigneaud A. Recherches sur la fovea de la retine humaine et particulie`rement sur le bouquet des cones centraux. Arch Anat Microsc 1907;9:315–342.
2. Yamada E. Some structural features of the fovea central in the human retina. Arch Ophthalmol 1969;82(2):151–159.
3. Gass JD. Müller cell cone, an overlooked part of the anatomy of the fovea centralis: hypotheses concerning its role in the pathogenesis of macular hole and foveomacular retinoschisis. Arch Ophthalmol 1999;117(6):821–823.
4. Syrbe S, Kuhrt H, Gärtner U, et al. Müller glial cells of the primate foveola: An electron microscopical study. Exp Eye Res. 2018;167:110-117.
5. Govetto A, Bhavsar KV, Virgili G, et al. Tractional Abnormalities of the Central Foveal Bouquet in Epiretinal Membranes: Clinical Spectrum and Pathophysiological Perspectives. Am J Ophthalmol. 2017;184:167-180.
6. Ramon Y Cajal S. Histologie du Système Nerveux de l'Homme et des Vertébrés, Paris, 1909–1911.
7. Bringmann A, Wiedemann P. Müller glial cells in retinal disease. Ophthalmologica. 2012;227(1):1-19.
8. Govetto A, Dacquay Y, Farajzadeh M, et al. Lamellar Macular Hole: Two Distinct Clinical Entities? Am J Ophthalmol. 2016;164:99-109.
9. Figueroa MS, Ruiz-Moreno JM, Gonzalez del Valle F, et al. Long-term outcomes of 23-gauge pars plana vitrectomy with internal limiting membrane peeling and gas tamponade for myopic traction maculopathy: a prospective study. Retina. 2015;35(9):1836-1843.
10. Li M, Nuisingh C, Messinger J, Dolz-Marco R, Ferrara F, Freund KB, Curcio CA. Histology of geographic atrophy secondary to age-related macular degeneration: a multilayer approach. Retina. 2018;38(10):1937-1953.
11. Bringmann A, Syrbe S, Görner K, et al. The primate fovea: Structure, function and development. Prog Retin Eye Res. 2018;66:49-84.
12. Polyak, SL, Klüver, H. The vertebrate visual system. Chicago: University of Chicago Press, 1957.
13. Perry, VH, Cowey, A. The lengths of the fibres of Henle in the retina of macaque monkeys: implications for vision. Neuroscience 1988;25(1):225-236.
14. Distler C, Dreher Z. Glia cells of the monkey retina--II. Müller cells. Vision Res. 1996;36(16):2381-2394.

15. Burris C, Klug K, Ngo IT, Sterling P, Schein S. How Müller glial cells in macaque fovea coat and isolate the synaptic terminals of cone photoreceptors. J Comp Neurol. 2002;453(1):100-111.

16. Mamballikalathil, I., Mann, C, Guidry C. Tractional force generation by porcine Müller cells: stimulation by retinal pigment epithelial cell-secreted growth factor. Invest Ophthalmol Vis Sci 2000;41(2):529-536.

17. Guidry C, Bradley KM, King, JL. Tractional force generation by human Müller cells: growth factor responsiveness and integrin receptor involvement. Invest Ophthalmol Vis Sci 2003;44(3):1355-1363.

18. Guidry C. The role of Müller cells in fibrocontractive retinal disorders. Prog Retin Eye Res 2005;24(1):75-86.

19. Guidry C, King JL, Mason JO 3rd. Fibrocontractive Müller cell phenotypes in proliferative diabetic retinopathy. Investigative ophthalmology & visual science 2009;50(4):1929-1939.

20. King JL, Guidry C. Vitreous IGFBP-3 effects on Müller cell proliferation and tractional force generation. Investigative Ophthalmology & Visual Science 2012;53(1): 93-99.

21. Lu YB, Pannicke T, Wei EQ, et al. Biomechanical properties of retinal glial cells: comparative and developmental data. Exp Eye Res. 2013;113:60-5.

22. Figueroa MS, Noval S, Contreras I. Macular structure on optical coherence tomography after lamellar macular hole surgery and its correlation with visual outcome. Can J Ophthalmol. 2011;46(6):491-7.

23. Lu, Y.B., Iandiev, I., Hollborn, M., Körber, N., et al. Reactive glial cells: increased stiffness correlates with increased intermediate filament expression. FASEB J. 2011;25(2):624–631.

24. Bringmann, A., Iandiev, I., Pannicke, T., et al. Cellular signaling and factors involved in Müller cell gliosis: neuroprotective and detrimental effects. Prog. Retin. Eye Res. 2009;28(6):423–451.

25. Drasdo N, Millican CL, Katholi CR, Curcio CA. The length of Henle fibers in the human retina and a model of ganglion receptive field density in the visual field. Vision Res. 2007;47(22):2901-2911.

26. Schein S. Anatomy of the macaque fovea and spatial densities of neurons in the foveal representation. Journal of Comparative Neurology 1988;269(4):479–505.

27. Popovic Z, Sjöstrand J. The relation between resolution measurements and numbers of retinal ganglion cells in the same human subjects. Vision Research 2005;45(17):2331–2338.

28. Franze K, Francke M, Günter K, et al. Spatial mapping of the mechanical properties of the living retina using scanning force microscopy. Soft Matter 2011;7:3147-3154.

FIGURE CAPTIONS

Figure 1: Simplified representation of foveal and parafoveal Müller cells. Parafoveal Müller cell is depicted as a solid structure composed of three rigid segments, R1, R2, and R3, of different lengths L1, L2 and L3. R1 and R3 are connected to R2 through two elastic hinges, which can rotate. The base of R3 is clamped and represent the external limiting membrane (ELM). The top end of R1 cannot rotate and represent the internal limiting membrane (ILM). The angle θ is comprised between the horizontal projection of R2 and the vertical projection of R1 and R3. Foveal Müller cell is depicted as vertical segment R of length L, clamped at its bottom (ELM) and with its top corresponding with the ILM. **Left. Relaxed parafoveal Müller cell.** In a relaxed configuration such as that depicted, R2 is completely horizontal, and the amplitude of angle θ is maximum (90°). **Middle-Left. Beveled parafoveal Müller cell.** Under the action of mechanical forces applied over the top of R1, the cell's segment R2 assumes a beveled configuration. Consequently, angle θ decreases (between 0 and 90°). **Middle-Right. Vertical parafoveal Müller cell.** Persistent and/or higher mechanical forces may cause the complete verticalization of parafoveal Müller cells. R1, R2 and R3 are vertically aligned, and the amplitude of angle θ is minimal (0°). **Right. Foveal Müller cell.** The morphology and behavior of foveal Müller cells is similar to that of a vertical parafoveal Müller cell.

Figure 2: Quantitative spectral-domain optical coherence tomography measurements. The schitic "bridges" of tissue were assumed to correspond to the R2 segment of the modeled parafoveal z-shaped Müller cell. The R1 segment corresponded to a vertical line traced from the internal limiting membrane to the beginning of the R2 segment under the outer plexiform layer. The R3 segment corresponded to a vertical line traced from the end of the R2 segment below the Henle fiber layer to the external limiting membrane. R1, R2 and R3 lengths were measured and labelled L_1,L_2 and L_3. L_1, L_2 and L_3 were measured at 200, 500, 1000, 1500, 2000 and 3000µm nasally ant temporally to the fovea depending on the extension of the schitic lesion. In this example, the lesion extended from 500µm nasally to the fovea to 2000µm temporally to the fovea.

Figure 3: Müller cell stiffness variation according to θ. **Left.** Value of the cell stiffness $K(\theta)$ versus the angle θ, normalised with the corresponding value K obtained for $\theta = 90°$. **Right.** Force F, scaled with 2γ/L, as a function of the angle θ. The relaxed configuration of the cell corresponds to the case in which the three rods are at right angles ($\theta = 90°$).

Figure 4: Variation of Müller cell morphology in different macular tractional disorders. Top. Relaxed configuration in physiologic conditions. R2 segment is

horizontal, parallel to the retinal pigment epithelium (angle θ = 90°)**. Middle.** In tractional lamellar macular hole, R2 segment in beveled but not completely vertical (angle θ comprised between 0 and 90°). **Bottom.** In myopic foveoschisis R2 segment is completely vertical, perpendicular to the retinal pigment epithelium (angle θ = 90°).

Figure 5: Progression of myopic foveoschisis. This example illustrates the morphological evolution of a myopic foveoschisis case. **Left.** At presentation, the intraretinal bridges of tissue of the Henle fiber layer appear intact, visual acuity is good. **Middle.** Over the follow-up of three years, the bridges of tissue progressively elongated, but without a significant drop in visual acuity. The bridges appear preserved. **Right.** Al the end of the follow-up period, visual acuity significantly dropped in comparison to baseline and disruption of the intraretinal segments is visible. This may suggest possible presynaptic damage to the photoreceptor's axons.

Figure 6: Hypothesis on the behavior of parafoveal Müller cells under stress and relationship with visual function. Left. Relaxed configuration. Müller cell processes and photoreceptor's axon run in parallel in the Henle fiber layer. Photoreceptors make synapsis in the outer nuclear layer (OPL) with the bipolar cells. **Middle-Left.** Mechanical stress. Under mechanical stress, the Müller cells behave like elastic solids, progressively stretching over the action of mechanical forces. At the beginning, only a part of the cell verticalized while the remaining part remains horizontal. Photoreceptor's axons follow the course of the Müller cell process. **Middle-Right.** If the action of mechanical forces persists, the Müller cell assumes a completely vertical configuration, as well as the photoreceptor's axon. In this configuration, the cell's stiffness is maximal. **Right.** Stiffer Müller cell may not deform and may break under the action of mechanical forces. Breaks at this level may damage photoreceptor's axons which are unable to transmit the signal to the bipolar cells, potentially affecting visual acuity.

Table 1: Exclusion Criteria:

Exclusion Criteria	• Any previous intraocular surgery with the exclusion of uncomplicated phacoemulsification. • History of retinal detachment. • Age-Related Macular Degeneration. • History of Choroidal neovascularization of any etiology. • Central Serous Chorioretinopathy. • Proliferative Diabetic Retinopathy. • Non-Proliferative Diabetic Retinopathy with history of clinically significant diabetic macular edema. • Macular teleangectasias. • Tractional and Degenerative lamellar macular holes. • History of central or branch retinal vein occlusion and central or branch retinal artery occlusion. • Advanced Glaucoma, or optic neuropathy of any kind. • History of inflammatory eye disorders. • History of Irvine-Gass syndrome. • Visually significant cataract. • History of endophthalmitis or any other intraocular infection. • Retinal dystrophies. • Foveal hypoplasia/Fovea plana • History of ocular trauma. • Any other potential cause of vision loss other than epiretinal membrane and/or macular schisis.

Table 2

Qualitative SD-OCT analysis at baseline and at the end of the follow-up.

		Baseline	End of Follow-up
Presence of central R segment	Myopic foveoschisis (n=11)	8/11	8/11
	Tractional lamellar Macular Hole (n=85)	29/85	28/85
	p-value	*0.013*	*0.010*
Central EZ/ELM disruption	Myopic foveoschisis (n=11)	5/11	7/11
	Tractional lamellar Macular Hole (n=85)	1/85	1/85
	p-value	*<0.001*	*<0.001*
Parafoveal EZ/ELM disruption	Myopic foveoschisis (n=11)	5/11	6/11
	Tractional lamellar Macular Hole (n=85)	0/85	0/85
	p-value	*<0.001*	*<0.001*
Tractional abnormalities of the CB	Myopic foveoschisis (n=11)	4/11	2/11
	Tractional lamellar Macular Hole (n=85)	3/85	2/85
	p-value	*<0.001*	*<0.001*

EZ: Ellipsoid zone; ELM: External Limiting Membrane; CB: Central Bouquet.

Table 3: Baseline quantitative SD-OCT analysis: length of segments R, R1, R2 and R3.

	R (L) µm	R1 (L_1) µm						R2 (L_2) µm						R3 (L_3) µm					
Distance from the foveal center (µm)*	0-50	200	500	1000	1500	2000	3000	200	500	1000	1500	2000	3000	200	500	1000	1500	2000	3000
MF (n=11)	383 ±211	110 ±75	130 ±43	172 ±47	189 ±62	208 ±113	236 ±150	231 ±95	263 ±109	242 ±150	200 ±119	170 ±101	180 ±70	93 ±52	104 ±88	78 ±60	75 ±53	90 ±92	
TLMH (n=85)	156 ±87	119 ±43	171 ±44	188 ±37	178 ±17	157 ±53	-**	162 ±69	117 ±63	75 ±47	112 ±102	88 ±78	-**	92 ±26	85 ±23	80 ±33	74 ±14	59 ±11	-**
p-value	<0.001	0.070	0.060	0.080	0.970	-**	-**	0.001	<0.001	<0.001	0.02	-**	-**	0.700	0.167	0.190	0.200	-**	-**

MF: Myopic Foveoschisis; TLMH: Tractional Lamellar Macular Hole.

**Nasal and temporal measurements combined.*

***It was not possible to calculate p-values at 2000 and 3000µm due to the very low number of lesions in the tractional lamellar macular hole subgroup. There were no tractional lamellar macular holes with a schisis extending up to 3000µm from the foveal center.*

Table 4: Baseline quantitative SD-OCT analysis: angle θ assessment.

Distance from the foveal center (µm)*	200	500	1000	1500	2000	3000
MF	13±8°	12±10°	16±10°	14±11°	17±15°	8±4°
TLMH	32±14°	42±12°	43±15°	45±5°	45±7°	-**
p-value	*<0.001*	*<0.001*	*<0.001*	*<0.001*	-**	-**

MF: Myopic Foveoschisis; TLMH: Tractional lamellar macular hole.

* *Nasal and temporal measurements combined.*

***It was not possible to calculate p-values at 2000 and 3000µm due to the very low number of lesions in the tractional lamellar macular hole subgroup. There were no tractional lamellar macular holes with a schisis extending up to 3000µm from the foveal center.*

Figure 1

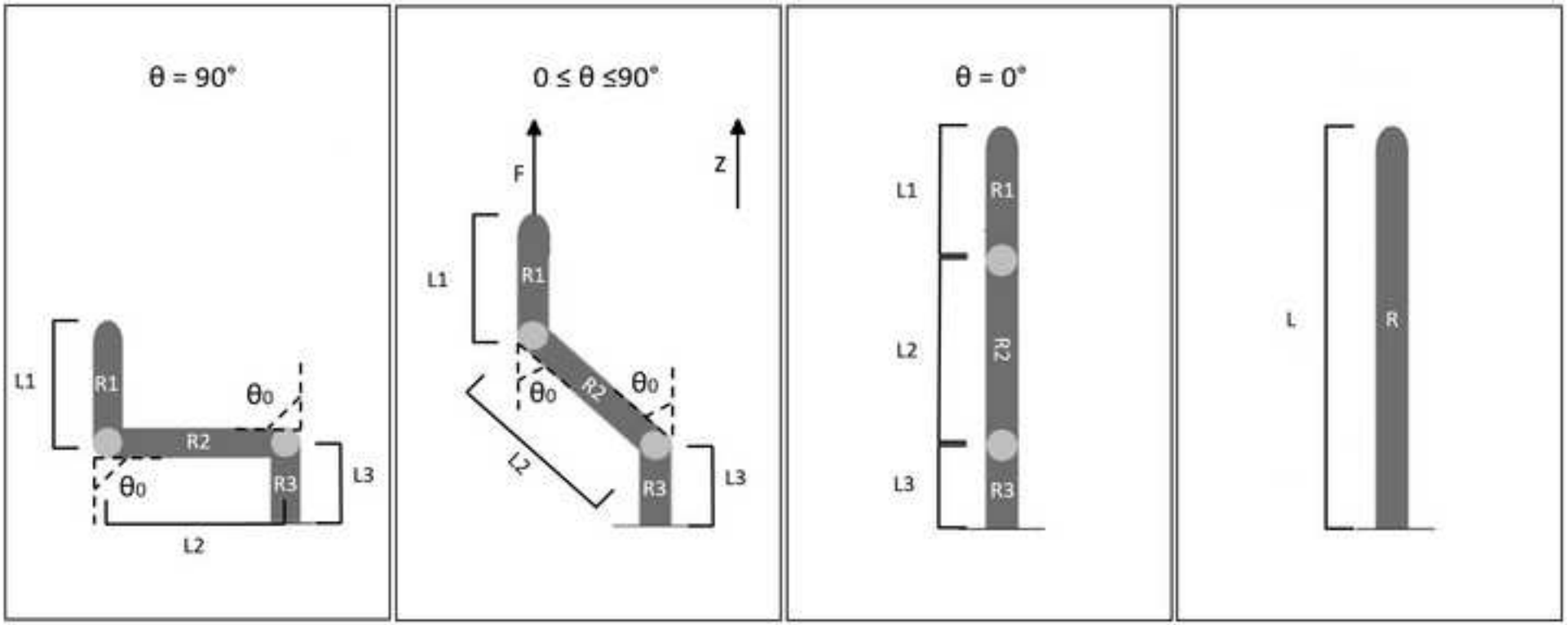
θ = 90°
L1
R1
θ0
R2
θ0
R3
L3
L2
0 ≤ θ ≤90°
F
Z
L1
R1
θ0
R2
θ0
L2
R3
L3
θ = 0°
L1
R1
L2
R2
L3
R3
L
R

Figure 2

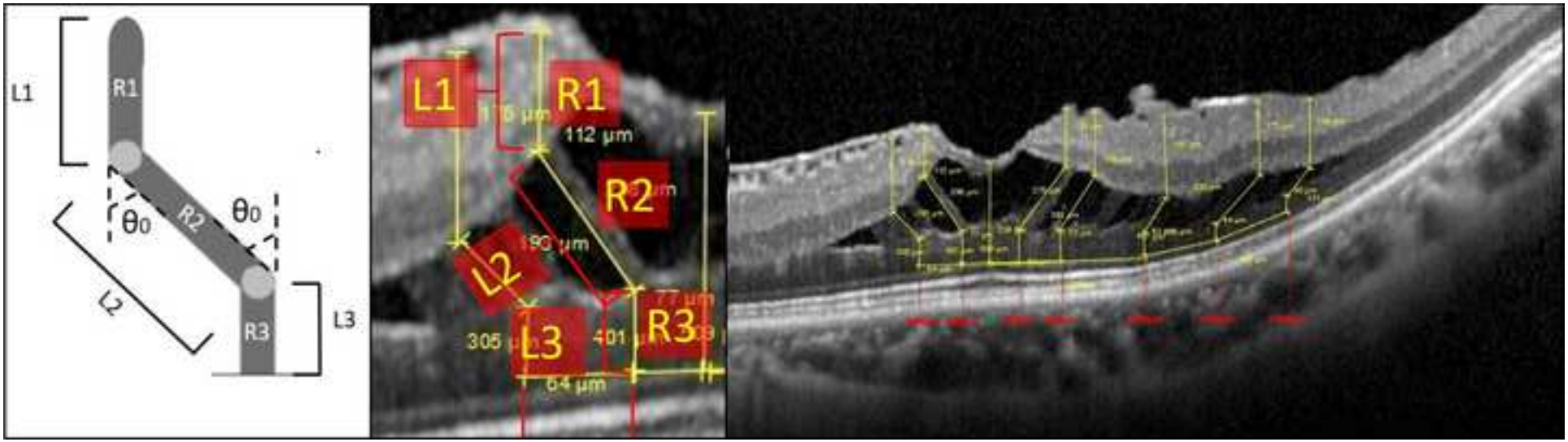
L1
R1
θ0
θ0
R2
L2
R3
L3
L1
R1
112 µm
R2
190 µm
L2
305 µm
L3
401 µm
R3
64 µm

Figure 3

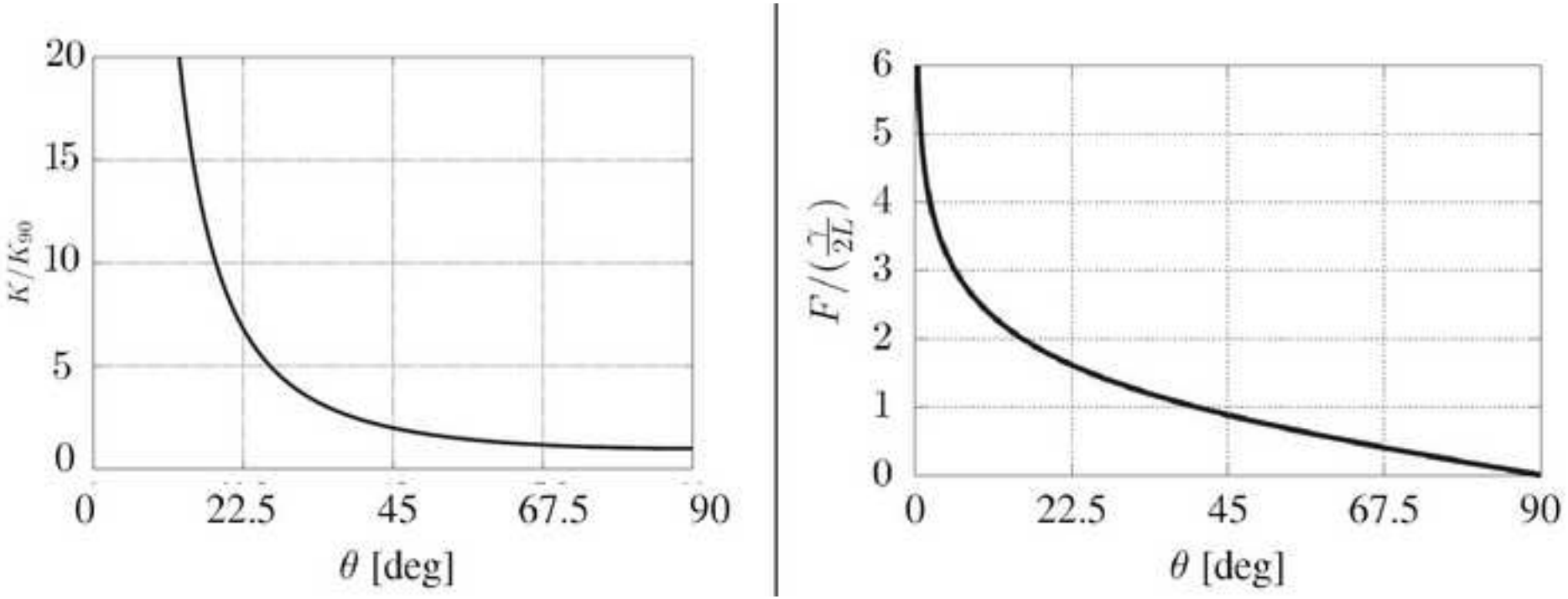
20
15
10
5
0
K/K_{90}
0
22.5
45
67.5
90
θ [deg]
6
5
4
3
2
1
0
$F/(\frac{\gamma}{2L})$
0
22.5
45
67.5
90
θ [deg]

Figure 4

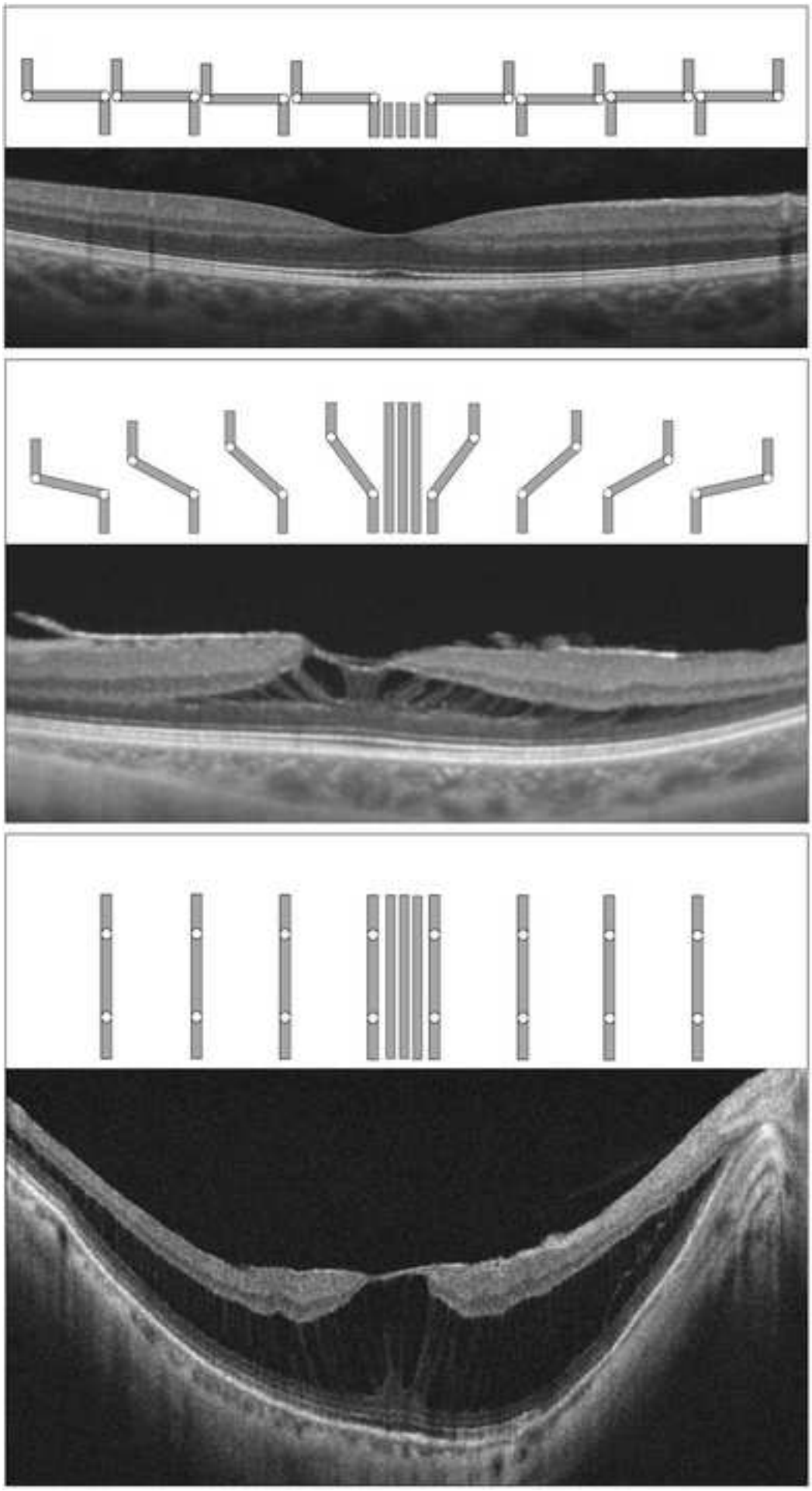

Figure 5

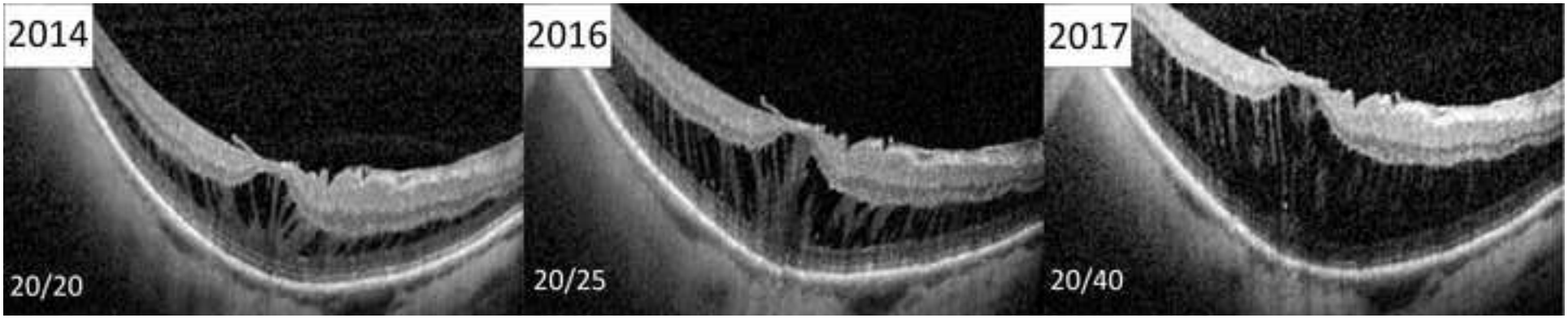

Figure 6

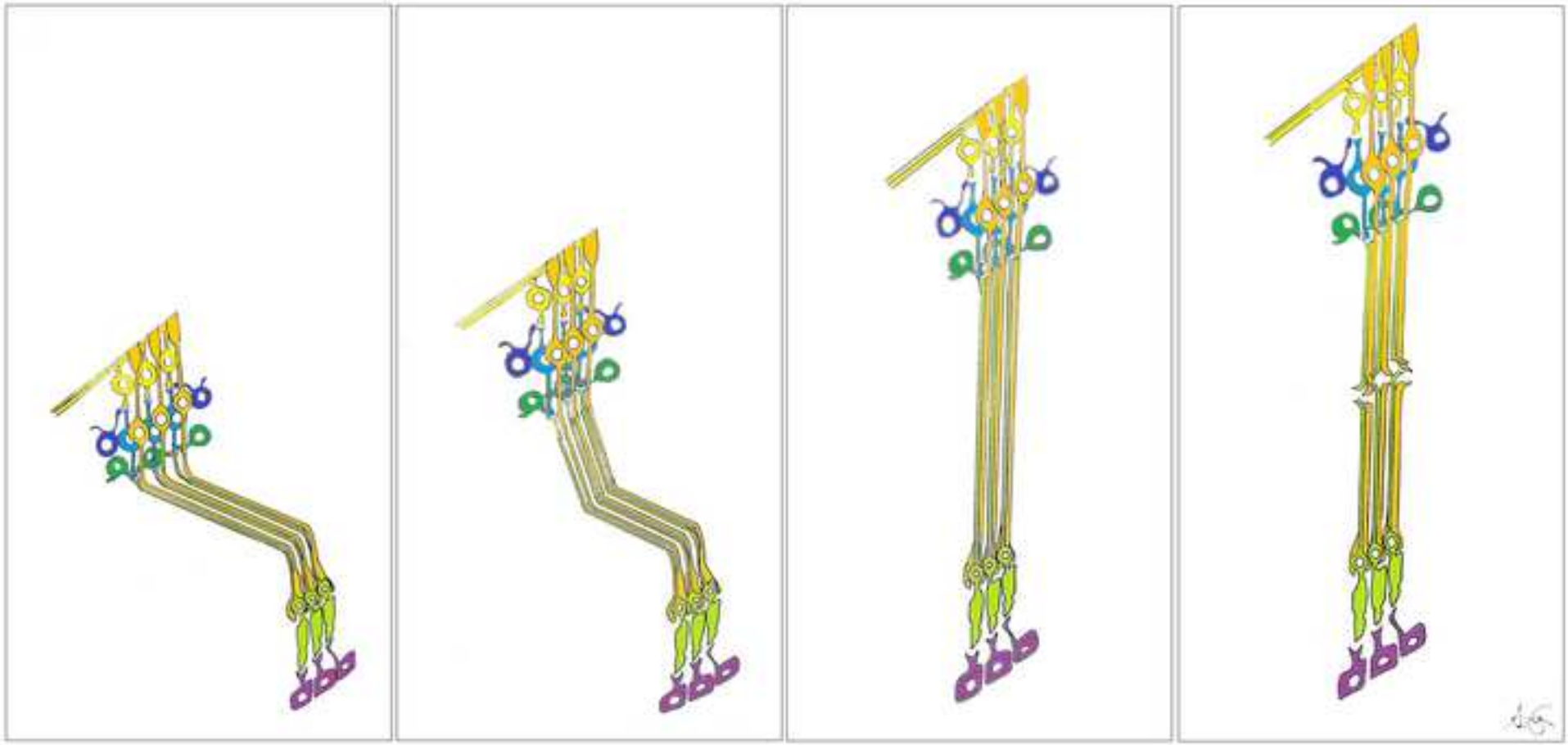

TABLE OF CONTENTS STATEMENT

Title: The role of Müller cells in tractional macular disorders: an optical coherence tomography study and physical model of force transmission.

Table of contents: This study explored the possible behavior of foveal and parafoveal Müller cells in response to mechanical forces with the development of a simple physical model of force transmission. The stiffness of the Müller cells may dramatically increase at decreasing values of angle θ, which may translate in higher mechanical force transmission to photoreceptors. Such results suggest the key role of Henle fiber layer in maintaining structural stability of the parafovea.

BIOSKETCH

Andrea Govetto, MD, PhD is a vitreo-retinal specialist at the Oftalmico Hospital in Milan, Italy. He completed an international fellowship in vitreoretinal diseases and surgery research at the Stein Institute, University of California, Los Angeles. Dr. Govetto has authored several publications in peer-reviewed journals and his clinical and research interests focus particularly on the disorders of the vitreo-retinal interface and retinal imaging.